

Chapter 14

Optimization of Planocentric Gear Train Characteristics with CA-Tools



Gorazd Hlebanja, Miha Erjavec, Simon Kulovec and Jože Hlebanja

Abstract The planocentric gearboxes are characterized by the coaxial input and output shafts and large transmission ratios, which can be achieved based on a ring gear with internal gearing in combination with usually two planet gears with external gearing, where the difference in the numbers of teeth between the gear ring and the planet gears is small, preferably amounting one. The proposed solution is based on the S-shaped tooth flank geometry. Since the required gear train characteristics impose strict limitations (e.g. near zero backlash) on the assembled product, it is necessary to simulate its tolerance behaviour. So, a professional or proprietary developed CA tools are necessary to deal with such analyses, e.g. KissSoft. Properties of a such gear train can be successfully modified in this way. A sophisticated testing rig was developed to verify actual gear train characteristics, and to test its short-term and long-term behaviour. Backlash, stiffness, kinematic error, and dynamic behaviour of produced gear trains are measured in this way.

Keywords Planocentric gear train · Backlash · Tolerance analysis · S-gearing

G. Hlebanja (✉)

University of Novo Mesto, FME, Na Loko 2, 8000 Novo mesto, Slovenia
e-mail: gorazd.hlebanja@siol.net; gorazd.hlebanja@podkrižnik.si

G. Hlebanja · M. Erjavec · S. Kulovec

Podkrižnik d.o.o., Lesarska cesta 10, 3331 Nazarje, Slovenia
e-mail: miha.erjavec@podkrižnik.si

S. Kulovec

e-mail: simon.kulovec@podkrižnik.si

J. Hlebanja

University of Ljubljana, FME, Aškerčeva c. 6, 1000 Ljubljana, Slovenia
e-mail: joze.hlebanja@siol.net

© Springer Nature Switzerland AG 2020

V. Goldfarb et al. (eds.), *New Approaches to Gear Design and Production*,
Mechanisms and Machine Science 81,
https://doi.org/10.1007/978-3-030-34945-5_14

14.1 Introduction

Planocentric gear boxes are in technical use for many decades due to their main characteristic, which is reduction of rotational speed and accordingly increased torque in the smallest available volume. This type of device is used in aircraft, marine, robotics, and many other industries. The expected efficiency may be as high as 90% or more and gear ratios can achieve up to 160:1 in a single step configuration. Basic arrangements of this type are described in renowned references, e.g. Radzevich [1] and Niemann and Winter [2]. The available industrial solutions include *Sumitomo* cyclo gearboxes [3], *Spinea* drives [4], *Nabtesco* [5], *Onvio* [6] and many others. Gearings are usually cycloidal or lantern. Some solutions combine planetary gear train and a cycloidal stage with three eccentrics having origins in the centers of planets. Some other devices incorporate a threefold eccentric rotating three planets. Such gearboxes are more compact but also more complex. All producers claim near zero or zero backlash. There is also a strong patent activity all over the world, also in Russia and China. This indicates importance of the field. Some patented solutions comprise gear boxes of Sumitomo and Jtekt Corporation [7–9], etc. The expected characteristics are low hysteresis for accurate positioning, low lost motion, compact design, high torsional stiffness, low inertia, high efficiency, overload capacity, easy assembly, and lifetime lubrication. Some robot producers develop and produce in-house patented gearings, e.g. *Stäubli's* JCS reduction gear boxes [10], which improve the precision, dynamics, and service life of its robots and lower their maintenance.

Additionally, some additional features can be built into a device, such as accurate output shaft positioning and output torque sensorics, which enable incorporation of such devices in collaborative robot's arm joints.

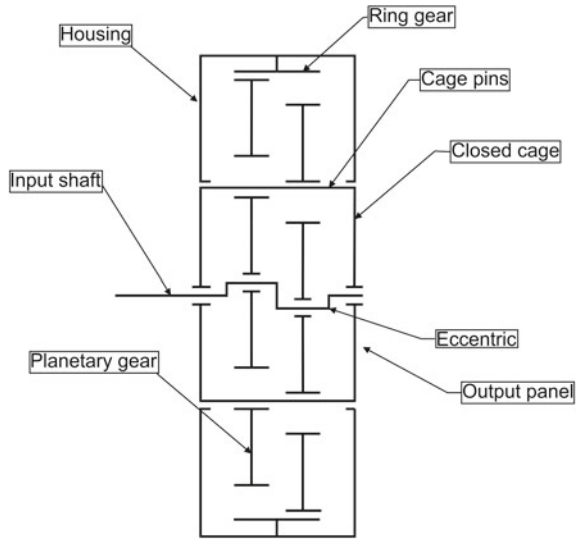
The paper presents kinematic circumstances of the proposed planocentric gear train. Some historical notes show basic mechanisms used in a contemporary gear train. The produced prototypes have been tested and results helped in improvements of new series. The comprehensive analysis in KissSoft helped in the design of new prototype, conforming to the requirements.

14.2 Kinematic Circumstances of a Planocentric Gear Train

The planocentric gearbox has coaxial input and output shafts, and large transmission ratios can be achieved based on a gear ring with internal gearing in combination with usually two planet gears with external gearing, where the difference in the numbers of teeth between the gear ring z_r and the planet gears z_p rules the gear ratio, Eq. (14.1). The difference in ring and planet numbers of teeth should be small, preferably amounting one.

$$i = \frac{z_p - z_r}{z_p} \quad (14.1)$$

Fig. 14.1 Scheme of double cage, double bearing planocentric gear box



The planet gears are mounted on an eccentric shaft, where bearings separate the planet gears from the eccentric. The planet gears wobble around the gear ring, that is, they reverse for one tooth in each revolution of the eccentric. The wobbling movement is in accordance with a hypocycloidal movement where the generating circle with the radius of the eccentric is rolling on the kinematic circle of the ring gear. And at the same time, the planet gear kinematic circle rolls in the inner side of the ring gear kinematic circle, which is simultaneous with the rotation of the eccentric. In this way the planetary gears develop rotation superimposed on the wobble. So, the input rotation of the eccentric is transformed into the reduced output rotation of the cage with the pins according to the gear ratio in the reverse direction of the input shaft in the same axis. And the gear ring is fixed to the housing. The planocentric gear train arrangement with a closed cage is illustrated in Fig. 14.1.

The eccentric driven planocentric gear train can be regarded as a simple mechanism with two links. The first link size is the radius of the eccentric and its joint indicates its position. The second one connects the eccentric with a point on the planet gear (a rigid body), e.g. the contact point. The eccentric link rotates and induces movement of the chosen point on the planet gear, which is restricted by a following rule:

$$r_v = r_p \frac{\varphi_p}{\varphi_g} \tag{14.2}$$

r_v and r_p are the radii of the kinematic circles of the gear and the planet gear, respectively. If the ring gear rotates for φ_v the planet rotates for φ_p .

A simple algorithm can be used to define movement of the planet based on the rotation of the eccentric and limited by Eq. (14.2) (Fig. 14.2).

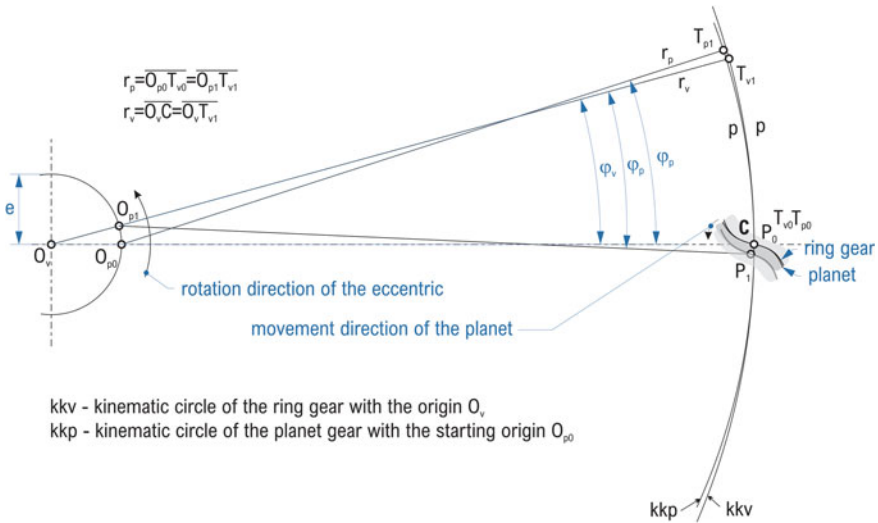


Fig. 14.2 Planetary gear movement in accordance with hypocycloid generated on the kinematic circle of the ring gear

- T_{p0} and T_{v0} coincide with C. P_0 is a point on the planet also coinciding with C.
- T_{p1} and T_{v1} are calculated according to Eq. (14.2). It is true: $p = \pi m = p = \pi m = \widehat{CT_{v1}} = \widehat{CT_{p1}}$.
- Eccentric turns for φ_v to the new point O_{p1} . kkp rolls on kkv in such a way that T_{p1} coincides with T_{v1} . So, tangents and normals of kkv and kkp coincide in T_{v1} .
- The normal of the planet in this point runs through O_v and O_{p1} .
- Since the planet is a rigid body, the right leg of the angle φ_p rotates around O_{p1} in CW direction for the difference $\Delta\varphi = \varphi_v - \varphi_p$.
- The procedure is continuous, but it can be numerically calculated by an adequate number of steps.

The above procedure can be formalized. Thus, successive points on the ring gear kinematic circle T_{vi} are defined as follows:

$$x_{T_{vi}} = r_v \cos \varphi_{vi} \text{ and } y_{T_{vi}} = r_v \sin \varphi_{vi}. \tag{14.3}$$

Similarly, successive position points O_{pi} of the eccentric are

$$x_{O_{pi}} = e \cos \varphi_{vi} \text{ and } y_{O_{pi}} = e \sin \varphi_{vi}. \tag{14.4}$$

And coordinates of the moving point P_i on the planet gear are

$$x_{P_i} = x_{O_{pi}} + r_p \cos \Delta\varphi_i \text{ and } y_{P_i} = y_{O_{pi}} + r_p \sin \Delta\varphi_i. \tag{14.5}$$

The planet gear tooth movement into a new ring gear tooth space is illustrated in Fig. 14.3 by 20 iterations. So, each point and planet gear position in Fig. (14.3) are based on successive rotations of the eccentric for 18° .

14.3 Historical Background

Potential advantages of planocentric gear boxes, namely a high-speed reduction ratio combined with high output torque in a relatively small volume, were a driving force for a new development already twenty years ago. So, the modified lantern gears were developed for use in planocentric gear drives with eccentric [11] and patented [12]. The internal gear pair during meshing is illustrated in Fig. 14.4, clearly indicating the value of eccentricity.

The teeth of the ring gear are designed as semi-circular extremities, whereas the planetary gears are designed with corresponding semi-circular spaces, adapted in size for a tolerance. Design aims were focused in automatic production lines and CNC-machinery. The planocentric lantern gear box design was robust. The transmission of rotation from the planet gears through a pin composition to the output shaft was provided by a single sided cage with double bearing output shaft. Small series were produced with various gear ratios up to 100 and with various modules, down to $m = 0.5$ mm.

A lantern gear train assembly is represented in Fig. 14.5. Gear boxes of this type have been produced in various sizes and configurations to serve primarily wood cutting automation machines. Materials for gears included among others self-lubricating plastics for planet gears, despite through hardened steel with tensile strength of 900 N/mm^2 prevailed. The specific load k_{lim} for continuous working conditions in the latter case amounted up to 125 N/mm^2 , which implied the output torque of 100 Nm for the illustrated gear box with the gear ratio 100 and the module 1 mm and $z_{ring} = 101$ and $z_{planet} = 100$.

14.4 Gear Tooth Flank Geometry

Beside semicircular, many other gear flank geometries have been proposed for planocentric gear trains, all in search for an optimal geometry.

The involute gear shape can be used to compose a planocentric gear box. Park et al. [13] conducted a research with the goal to produce a robotic gear box in order to replace an existing cycloidal planocentric gearbox. The key point of this model was also regarded to be economic in manufacture due to little influence of a manufacturing and assembly errors.

However, due to possible gear interference, such gears exhibit rather high pressure angle α_w around 30° , and Δz cannot amount to less than 5, or 4 based on the condition that the numbers of teeth of pinion and ring gear are rather high, 167 and 171 in this

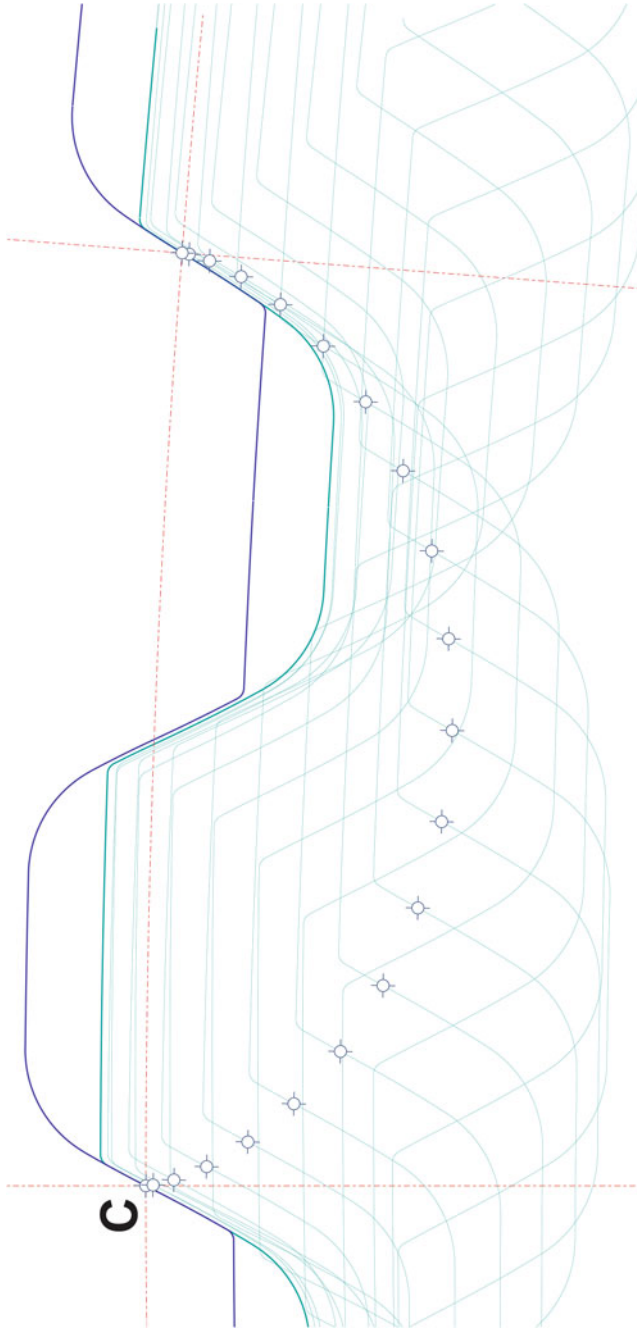


Fig. 14.3 Planetary gear movement in accordance with hypocycloid generated on the kinematic circle of the ring gear

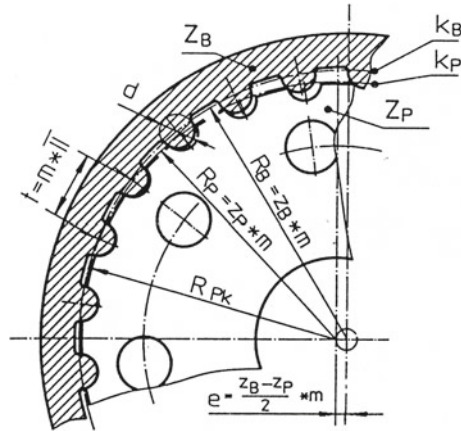


Fig. 14.4 Gear ring and planet gear during meshing

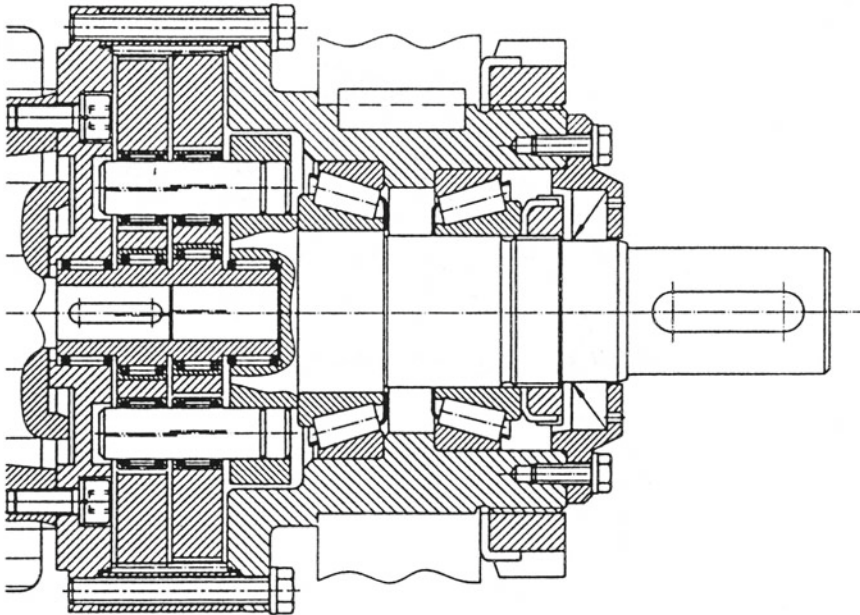


Fig. 14.5 Assembly of a robust planocentric lantern gear train

case. This also means essentially lower gear ratio (Eq. 14.1), $i^{-1} = 41.75$ for the above data.

Another attempt was made with a rectilinear tooth profile where a tooth is defined by two lines enclosing an angle, by an inside or outside circle, by the root circle and fillet arcs [14]. The power is transmitted by the arc at the pinion tooth tip which

slides over the linear tooth part of the gear ring. The problem is that such a gear composition does not follow the law of gearing. If a high-speed rotation is required, then such a gear arrangement can develop high noise and torque fluctuation.

Yet another tooth design is trapezoidal [15], where the contact of teeth is surface-like. However, the efficiency of such gear box may be poor, due to lack of rolling, amount of sliding and (non)conformity to the law of gearing.

A proposed solution is based on S-shaped tooth flank geometry for the meshing ring gear and planetary gears of the planocentric gear box. General ideas about S-gears have been described in several papers, e.g. [16–18].

The S-gear configuration has several advantages, the most important being the following:

1. Convex-concave contact in the vicinity of the meshing start and meshing end point;
2. Low amount of sliding during meshing which is due to the curved path of contact;
3. Evenly distributed flank load, which is due to similar sizes of addendums and dedendums of both meshing gears.

The other features include better lubrication due to high relative velocities and amount of rolling. In the case of internal-external gear pair some features may become less pronounced. Additionally, the path of contact is less curved, which is on behalf of smaller dedendum and addendum heights. However, S-gear shape is ruled by two parameters, the height parameter a_p and the curve exponent n . And by optimizing these two parameters one can shape this type of gearing in such a way to allow the gear and planet teeth number difference to be only one. So, it is possible design gear boxes with the diameter small diameters and high reduction ratios. The S-gearing for planocentric gear trains is illustrated in Fig. 14.6.

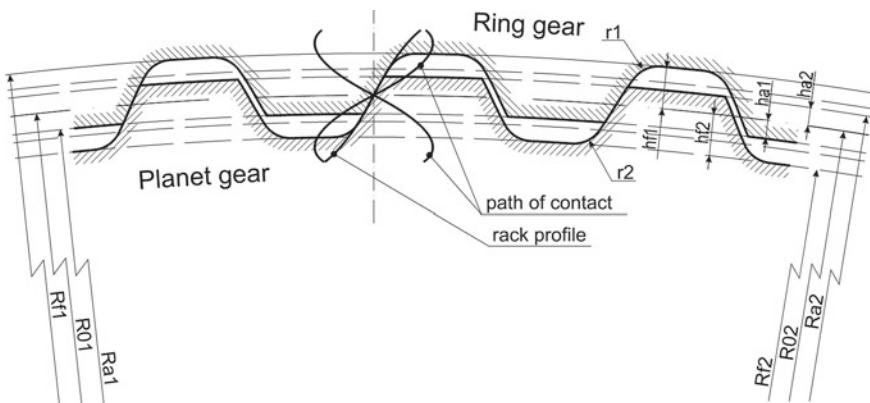


Fig. 14.6 S-gear flank geometry for the planocentric gear box

14.5 Planocentric Gear Box Prototypes

A small series of prototypes should be produced and assembled to test characteristics of a such gear box. The gear box is similar in function to those already mentioned. It contains an input shaft with eccentrics. As a motor rotates the shaft the eccentric rotates two planetary gears which wobble on the ring gear. The planetary gears are positioned in such a way that they enclose 180° for the sake of symmetry. Arrangements with three or more planetary gears are possible, which would impose high manufacturing skills regarding eccentrics. For each rotation of the eccentric the planetary gear proceeds for one tooth on the ring gear in the opposite direction. A cage consists of a supporting ring and output ring (serving also as the output shaft) that are connected by pins in an interference fit. The cage is rotated by planetary gears, having appropriate holes in which connecting pins with bearings comply. The cage is fixed to the input shaft by bearings at the extremities and in a similar manner to the housing with the ring gear. In this way a compact low volume gear box is achieved. It was decided that the device having module 1 mm, reduction ratio 80 ($z_v = 81$ and $z_p = 80$) and outer diameter around $\phi 100$ is the most interesting. The required maximal working torque is 120 Nm. The rendered image of this prototype is represented in Fig. 14.7 (from the input side) and the actual device in Fig. 14.8 (from the output side).



Fig. 14.7 Rendered image of the prototype planocentric gear box

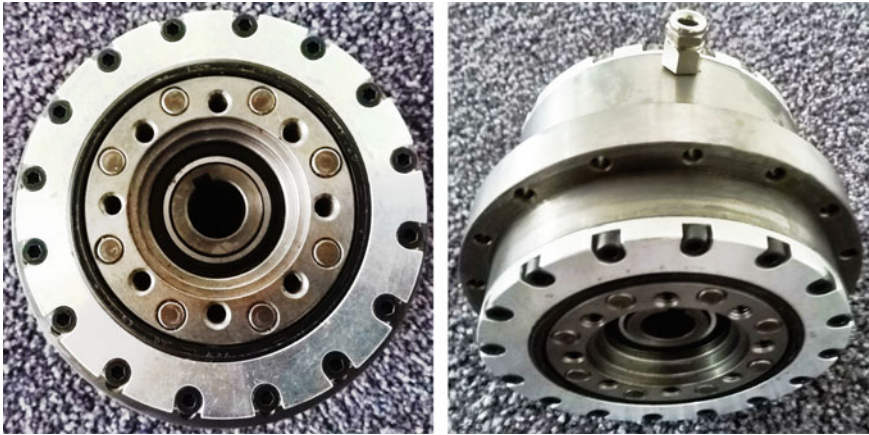


Fig. 14.8 Prototype planocentric gear box

Gear trains were tested, when assembled. Performed tests were backlash, hysteresis and stiffness, kinematic error, vibrations and noise, and durability tests. Special testing rigs were prepared or manufactured for testing of this type and similar devices. After that, the devices were disassembled, and components inspected on a CMM (Computerized measurement machine) and optically. Some typical testing results are presented below.

Since the device is intended for precision industry and robotics, its backlash and stiffness characteristic become crucial. The characteristic should be symmetric, regardless of any initial position of the planets and rotation direction, and the backlash in very narrow limits, <1 arcmin. As Fig. 14.9 indicates, the specimen 04 reveals backlash of 9 arcmin and stiffness characteristic which becomes considerably stiffer with increasing load. Stiffness of this device in the zone 3–50 Nm is 10 Nm/arcmin, in the zone 50–100 Nm 30 Nm/arcmin and 16Nm/arcmin in the zone 3–100 Nm. This gear train has actually higher values of stiffness, since the working torque limit amounts to 120 Nm. Similar gear train of *Spinea* (Spinea TS110) with gear ratio 89 has stiffness of 22 Nm/arc min. Sumitomo Cyclogear drive A15 with ratio 89 is a bit stronger drive has stiffness values as follows: 15 Nm in 3–50%, 28 Nm/arcmin in 50–100%, and 20 Nm/arcmin in the segment 3–100%.

Kinematic error of a gear train is defined as a deviation of the actual angular position from the theoretical angular position:

$$\Delta\varphi = i \cdot \varphi_{inp} - \varphi_{out} \quad (14.6)$$

Rotation of the input shaft (φ_{inp}) is measured with a 16-bit incremental encoder, whereas the output shaft (φ_{out}) rotation is measured by a built in absolute optical encoder with a high resolution. The optical encoder and the reading head are mounted with some tolerance, which reflects in a sinusoid carrying actual error signal. Several measurements of the kinematic error of the specimen 04, Fig. 14.10, yield maximal

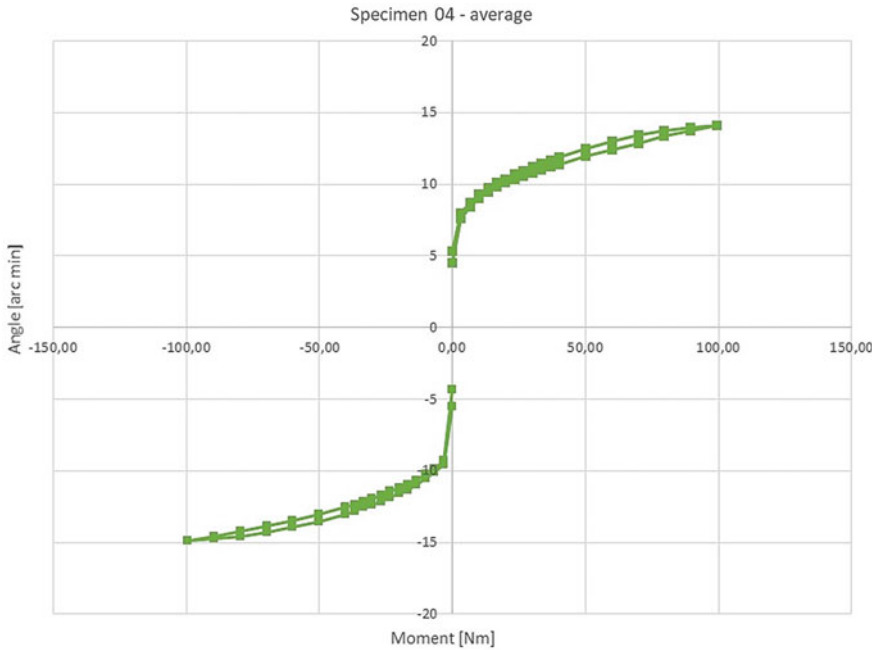
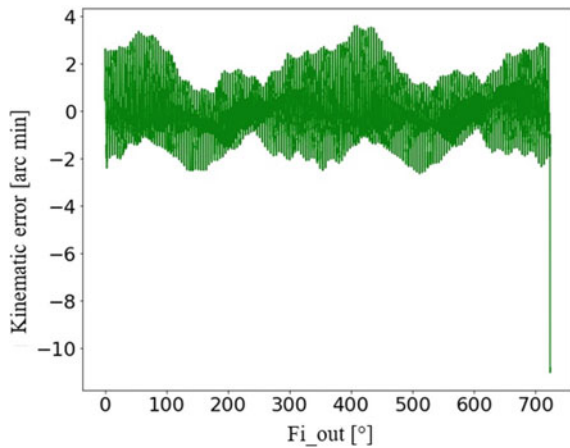


Fig. 14.9 Average of backlash and stiffness measurement of a specimen 04

Fig. 14.10 Kinematic error of a specimen 04



error limit of 6 arcmin.

Figure 14.11 shows the ring gear and the planets of the specimen 01 after disassembly. The specimen was submitted to high torques and speeds. The planet gears were made of 42CrMo4 and the ring of 25CrMo4, all gears plasma nitrided to HV700. The gears were carefully examined by an optical microscope. Gear teeth did not show

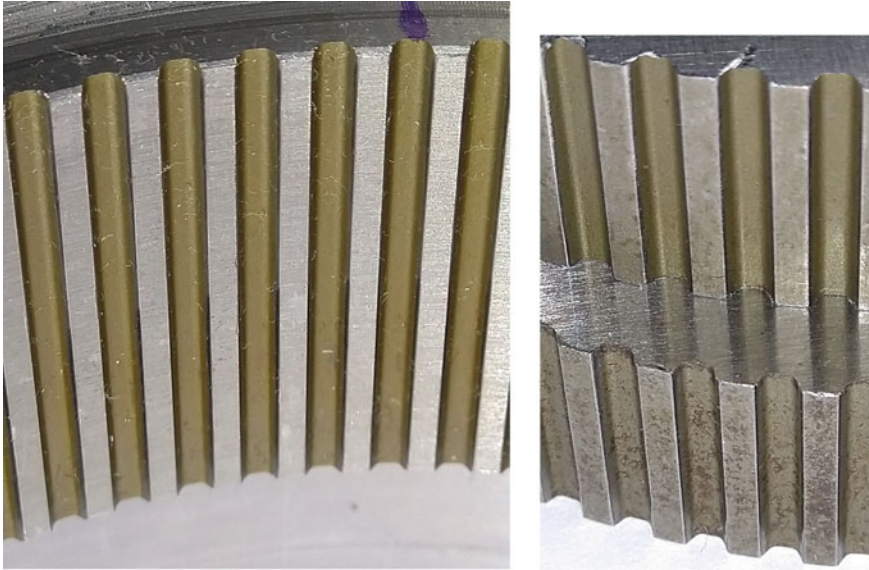


Fig. 14.11 Ring gear and planets of a specimen 01 after disassembly

any wear or damages. Initial wear appeared in some planet teeth tips and at certain locations in teeth tips. The reason is in meshing errors, which was discovered by measuring teeth spaces of the planets and the ring gear with a CMM.

In general, it could be concluded that first prototypes did not yet meet all prescribed requirements. So, it is necessary to improve the design and the quality of manufacturing so, that all measures are within prescribed tolerances. And with regard, So, all components should be inspected by the CM machine. Regarding gearing, the nominal circumferential backlash should be as low as possible, i.e. less than $10\ \mu\text{m}$, having manufacturing tolerance in the range of $5\ \mu\text{m}$. The circumferential arc of $10\ \mu\text{m}$ for the radius $40.5\ \text{mm}$ gives the angle of $0.85\ \text{arcmin}$ for geometrically precise circumstances.

14.6 Influences of Tolerances

This imposes the necessity to analyze influences of tolerances in varying circumstances. Such an analysis could disclose additional measures which would enable a convergence of the design towards accomplishing design requirements. As a primary tool for this task, the KissSoft [19] system was employed. KissSoft is software for effective, high-quality tool for calculating machine elements, reviewing these calculations, determining component strength, and documenting safety factors and product life parameters, incorporating currently valid standards (DIN, ISO, AGMA).

However, KissSoft uses the prevailing involute gear geometry. So, the first aim is to adapt geometry in such a way to reflect S-gear geometry. The current *KissSoft* User manual [20] includes possibility of a progressive profile modification (p. 343 of the named manual), which can be used as a modification in the addendum and the dedendum of a gear tooth, and is defined as follows:

$$\Delta_{ad} = 2 \cdot C_{ad} \cdot \left(\frac{d - d_k}{d_t - d_k} \right)^{f_{ad}/5} \quad \text{and} \quad \Delta_{dd} = 2 \cdot C_{dd} \cdot \left(\frac{d - d_k}{d_v - d_k} \right)^{f_{dd}/5} \quad (14.7)$$

Δ_{ad} and Δ_{dd} stand for a profile modification function in addendum and dedendum. C_{ad} and C_{dd} are modifying tip relief (or corresponding active dedendum modification) and f_{ad} and f_{dd} power coefficients. If a coefficient amounts to 5 the relief is linear. d_t , d_v , d_k , and d , are diameters of the tip circle, dedendum circle, kinematic circle and current circle. One can adapt the involute flank addendum and dedendum to S-gear flank. Such a modification is justified since addendum and dedendum heights are rather small, between 0.2 and 0.25 m .

So, a tolerance analysis of key elements and their mutual influences on functional properties of the gear train becomes possible. A theoretical analysis of various tolerance combinations of the gearing and their effects is presented was conducted. And subsequently influences of tolerances in bearings and assembly of connected shafts was studied, which can have a negative influence on the function of the gear box in certain working conditions. To prevent the planned function of the gear box, the backlash should be kept below 1 arcmin = 0.016°.

The aim is also to create a method of manufacturing and assembly, which would ensure the required precision and at the same time the tooth thickness tolerance would not be less than class h25, DIN3967 and the axis distance tolerance lesser than js6 (± 0.003) is not allowed in the KissSoft system.

14.6.1 Gearing Tolerances (Analysis of Tolerance Influences)

Figure 14.12 shows a computational shape of the used S-gears in the form of deviations from the involute gears. The planet gear was additionally modified with crowning amounting to 2 μm , as to prevent possible numerical singularities. This has a positive effect on a simulation. And in manufacturing, a worker at the machine is thus warned that the tooth cannot be concave and that the lead line should be straight or at least convex.

Initial state

The lowest backlash is 0°, but this can only be achieved if gears are manufactured on the higher tooth thickness limit, and at the same time the eccentricity is higher than nominal. For gears and eccentricity in the mean tolerance values the backlash amounts already to 0.062°.

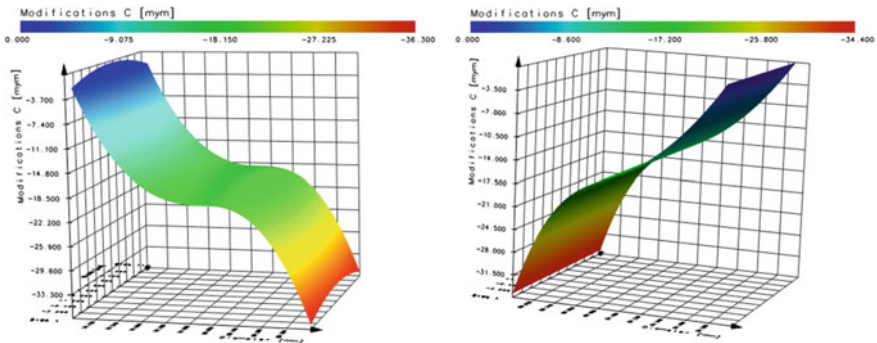


Fig. 14.12 S-gear data as they deviate from involute gearing (planet gear—left, ring gear—right)

Gears in production can be sorted in two classes based on the tooth thickness measurements. Values are collected in Table 14.1.

If a planet gear which is in the lower half class of the tooth thickness and a ring gear in the upper half class of the tooth thickness (Table 14.1, column 2), the backlash below the limit 0.016° cannot be achieved. The situation is almost identical with a combination thicker planet teeth and thinner ring gear teeth (column 3). If both, the planet and the ring gear tooth thickness are in the upper class, the limit 0.016° can be exceeded as well (column 4). So, one can conclude, that the chosen gear tooth thickness tolerances and the nominal axis distance with a selected tolerance do not lead to a gear box assembly complying to a basic functional requirement.

Table 14.1 Collected backlash limits for sorted gears in the nominal range (The effect of the angle of a planet rotation is insignificant.)

Backlash	Planet lower/ring upper	Planet upper/ring lower	Planet upper/ring upper
Highest	0.096	0.097	0.067
Mean	0.063	0.064	0.034
Lowest	0.029	0.031	0.000

Table 14.2 Collected backlash limits for sorted gears with shifted tolerance range (The effect of the angle of a planet rotation in the highest backlash range becomes notable and the backlash increases with the angle.)

Backlash	Planet upper/ring lower	Planet lower/ring upper	Planet lower/ring lower
Highest	0.011–0.012	0.0078–0.0082	0.036–0.037
Mean	0.000	0.000	0.004
Lowest	0.000	0.000	0.000

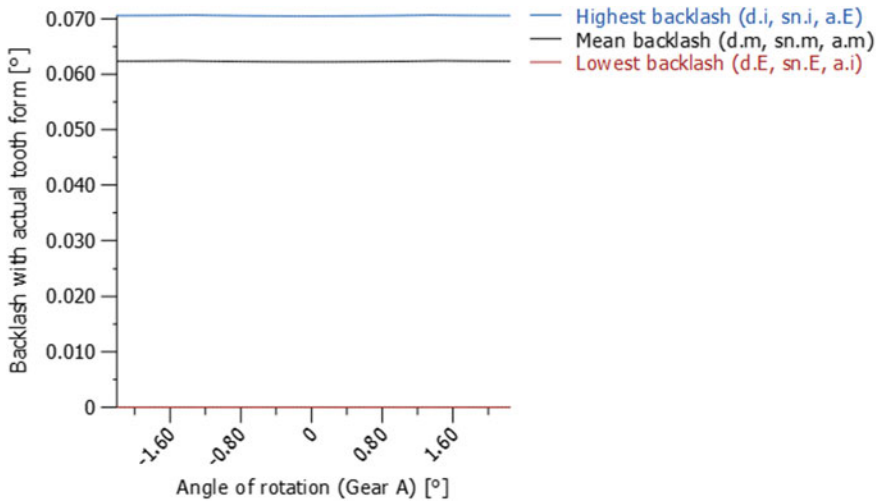


Fig. 14.13 Backlash (eccentricity 0.500js6; DIN3967 h25)

Shifted tolerance grade of the tooth thickness and increased axis distance

It is necessary to shift a tolerance grade of the tooth thickness or change the axis distance. Several iterations of the procedure described in the above sub-chapter lead to an acceptable solution.

So, the nominal axis distance increases from 0.500 to 0.520 mm and at the same time the tooth thickness tolerance is shifted for 0.020 mm towards thicker teeth for both, the planets and the ring gear (Fig. 14.13).

The highest backlash is reached for the lowest tooth thickness and axis distance values and its value (Fig. 14.14) is still above the allowable limit. Therefore, the method of discrimination of gears in two sub-groups based on tooth thickness will be used again. Values are collected in Table 14.2.

If a planet gear tooth thickness is from the upper part and the ring gear from the lower part of the tolerance grade the backlash is within prescribed limit (Table 14.2—column 2). The same is true for the reversed situation (Table 14.2—column 3). A logical conclusion is that if both, the planet and the ring gear, tooth thicknesses are in the upper part of the tolerance zone, an advantageous result is expected. If both gears are chosen from the lower part of the tolerance zone (Table 14.2—column 4), the result is similar as the results in mean value of the tolerance zone (Fig. 14.14), therefore unsatisfactory.

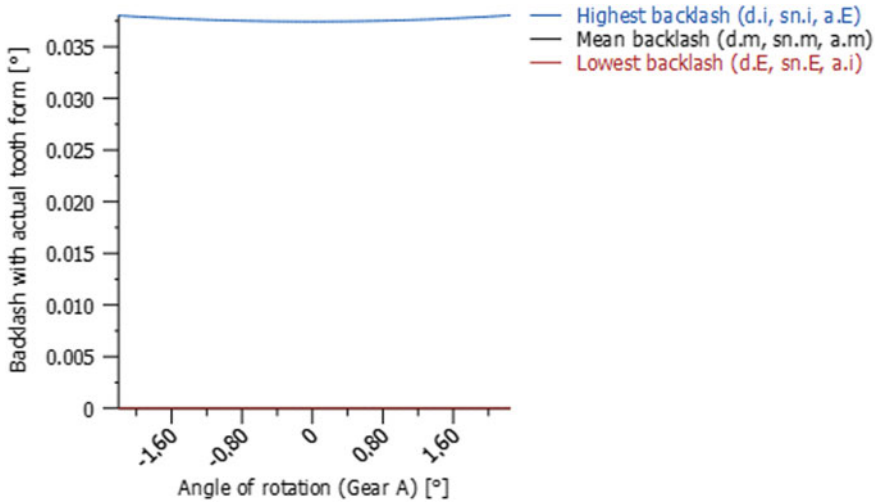


Fig. 14.14 Backlash (eccentricity 0.520js6; teeth tolerance shifted for 0.020 mm)

14.6.2 Contact Analysis

The load considered in contact analyses was prescribed working torque of 120 Nm at the output shaft. Several simulations were carried out with varying the axis distance and tooth thickness deviations. In this context, a transmission error as a function of the angle of rotation of the planet gear, a system stiffness in the contact zone and a contact pressure were simulated. And finally, a simulation of meshing of a planet gear with the ring gear is provided. The aim of the contact analysis is to discover possible interferences due to changes in the axis distance and tooth thickness values.

Several simulations were performed for both tolerance limits, that is for the eccentric and for the tooth thickness:

1. Axis distance 0.523 mm, tooth thickness deviation -0.020 mm (Fig. 14.15).
2. Axis distance 0.517 mm, tooth thickness deviation -0.020 mm (Fig. 14.16).
3. Axis distance 0.517 mm, tooth thickness deviation $+0.020$ mm (Fig. 14.17).
4. Axis distance 0.523 mm, tooth thickness deviation $+0.020$ mm (Fig. 14.18).

Transmission error is small, always in the range of less than 1 arcsec, the diagrams are presented exaggerated. The contact stiffness is in the range from 700 to 720 N/ μ m. And the contact pressure is in the range between 1100 and 1170 N/mm², which implies usage of heat-treated alloy steels. Furthermore, the meshing scheme shows that around five teeth pairs are always in contact. This was demonstrated also with a CAD kinematic analysis. It was also discovered that individual contact zones are rather small. This implies that only a short zone in the vicinity of the kinematic circles is actually active. And more important, no interferences resulted from these simulations.

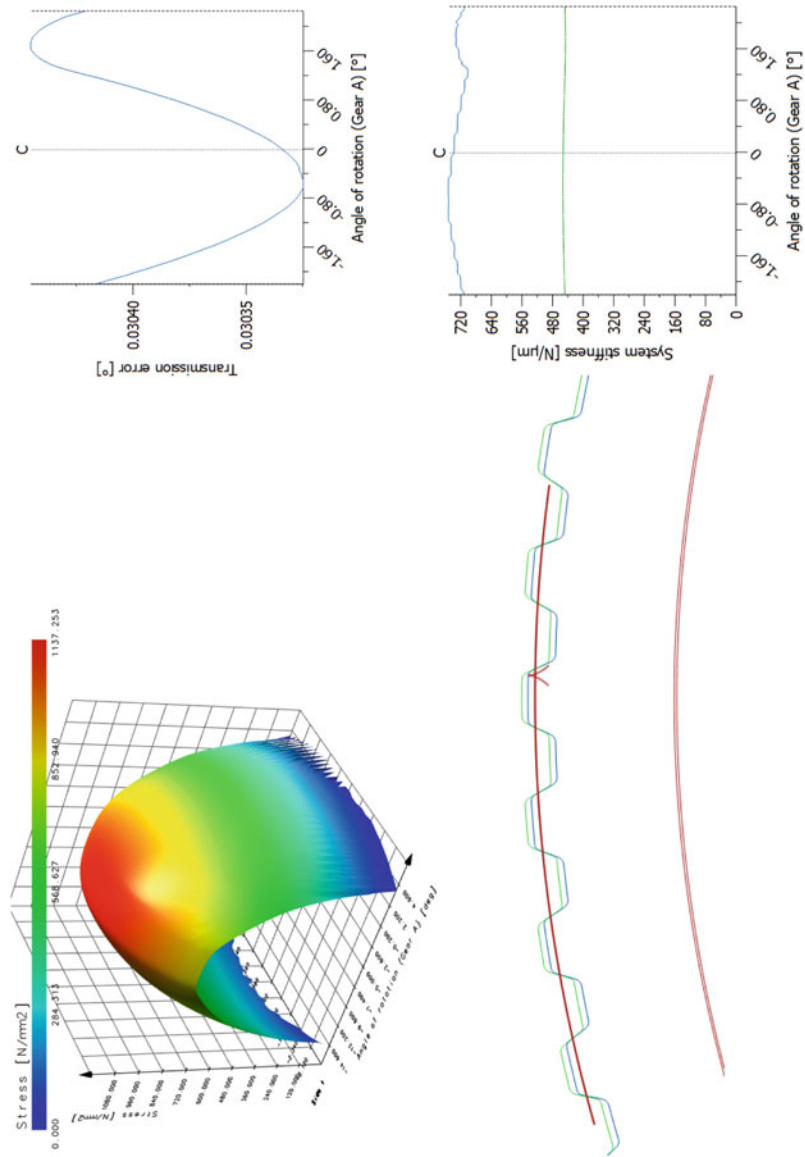


Fig. 14.15 Simulation with axis distance 0.523 mm, tooth thickness deviation -0.020 mm

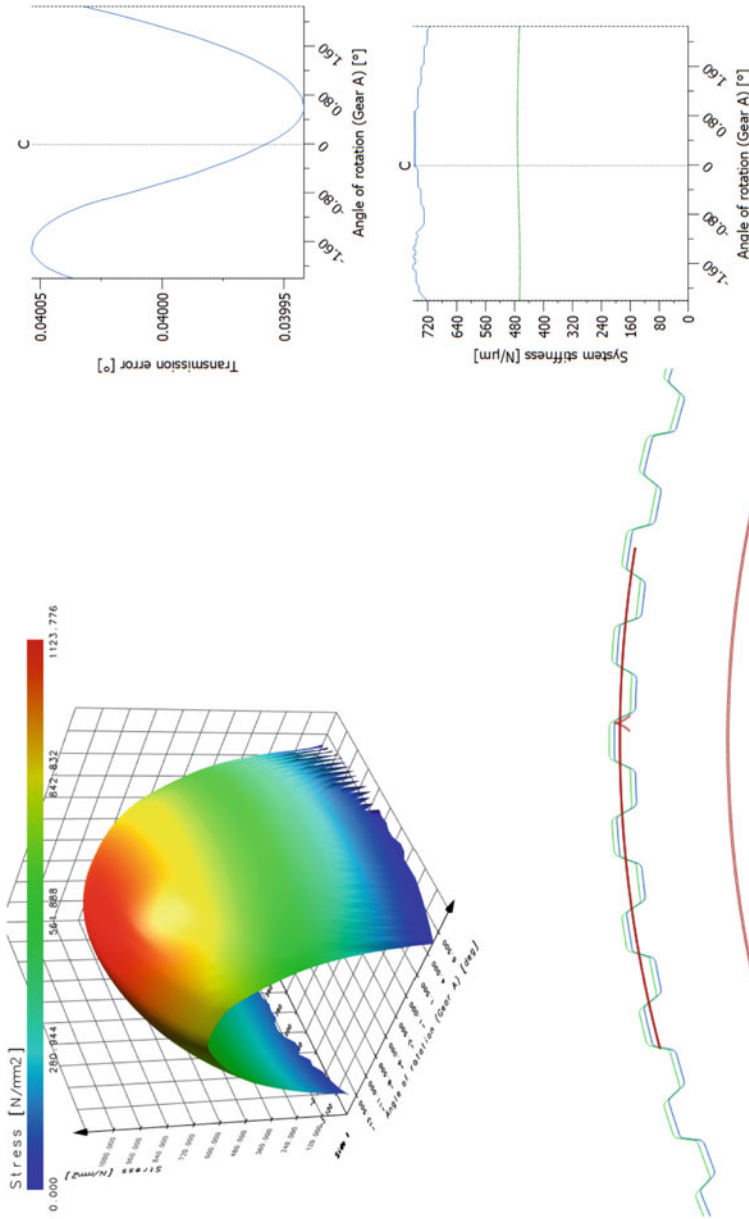


Fig. 14.16 Simulation with axis distance 0.517 mm, tooth thickness deviation -0.020 mm

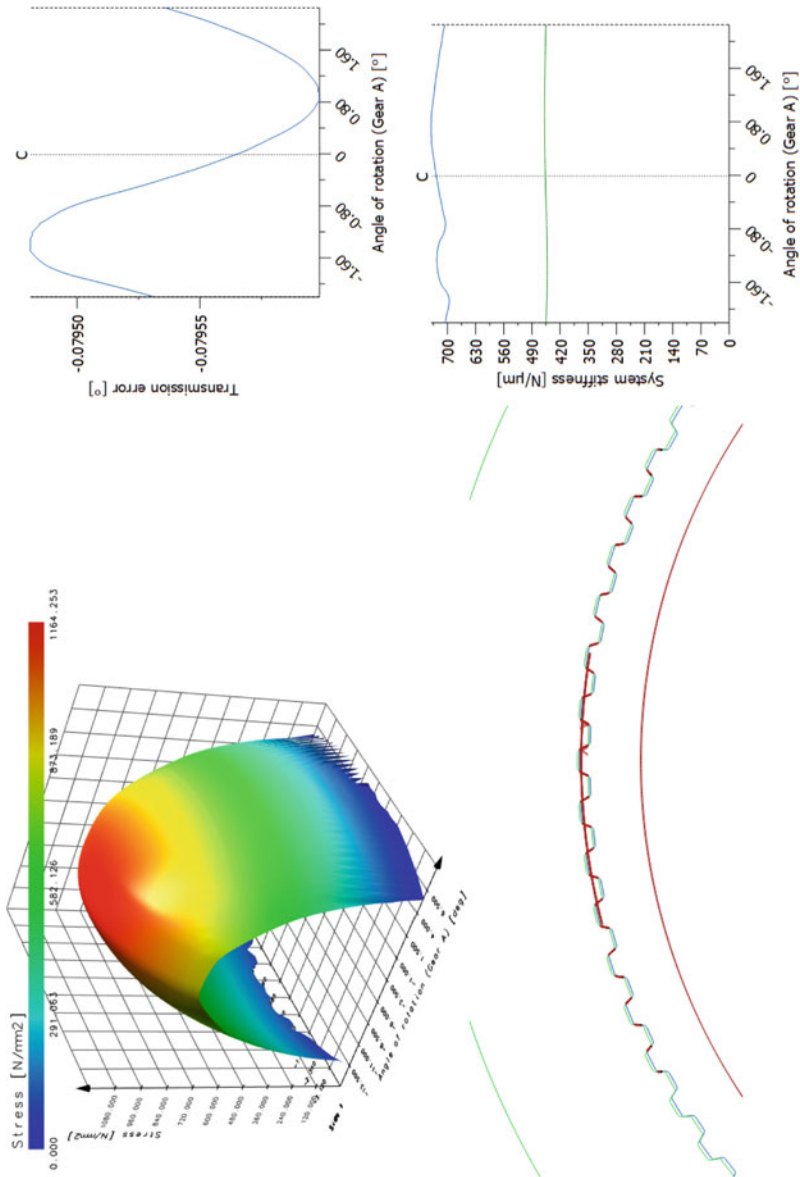


Fig. 14.17 Simulation with axis distance 0.517 mm, tooth thickness deviation +0.020 mm

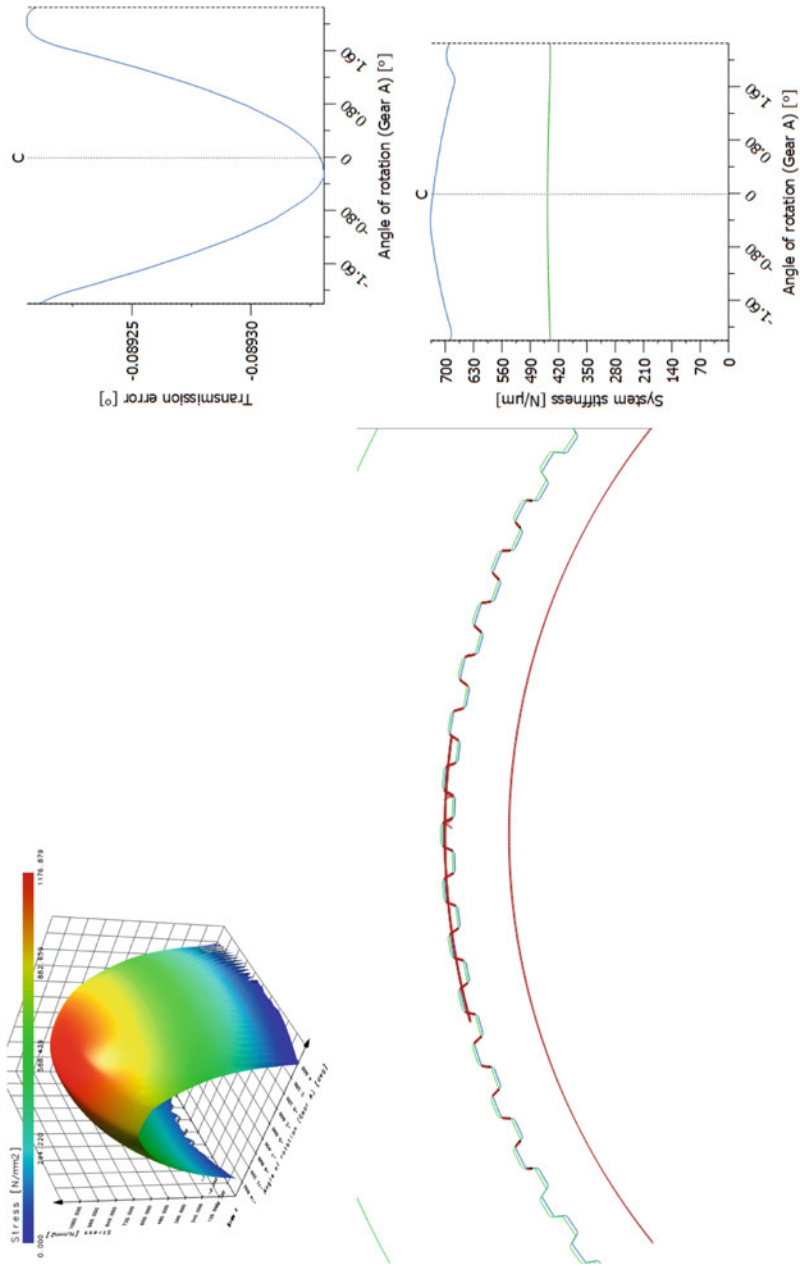


Fig. 14.18 Simulation with axis distance 0.523 mm, tooth thickness deviation +0.020 mm

14.6.3 Influence of Bearing Tolerances and Carriers on the Position of the Gear Train

The influence of carriers has not been considered in so far made calculations. That is why it is necessary to examine axis distance deviations emerging during operation under load (120 Nm). So, a model, clarifying deviations of a planet from its nominal position, was developed in KissSoft. The nominal position in the model amounts to 0 mm, which is due to easier simulation.

The situation illustrated in Fig. 14.19, shows an analysis for the case where for all bearing positions and clearances mean tolerance values are assumed. The axis distance changes for 0.007 mm in a direction towards increasing the backlash. So, if the eccentric is produced on the lowest tolerance limit 0.517 mm, the resulting eccentric link radius becomes 0.510 mm, which increases the backlash.

Assuming a possibility that bearing locations (shafts and housings bores) are made in such a way that these increase the deviation of the axis distance, as illustrated in Fig. 14.20, the axis distance deviation amounts to 0.015 mm and the axis distance 0.505 mm.

Such deviations with an additional displacement of the prescribed eccentricity on the other hand imply possible interference since the tolerances are narrow. So, the above analysis appears to be important in the context of functionality and detection of possible collisions between the ring gear and planet gears teeth tips. Figure 14.21

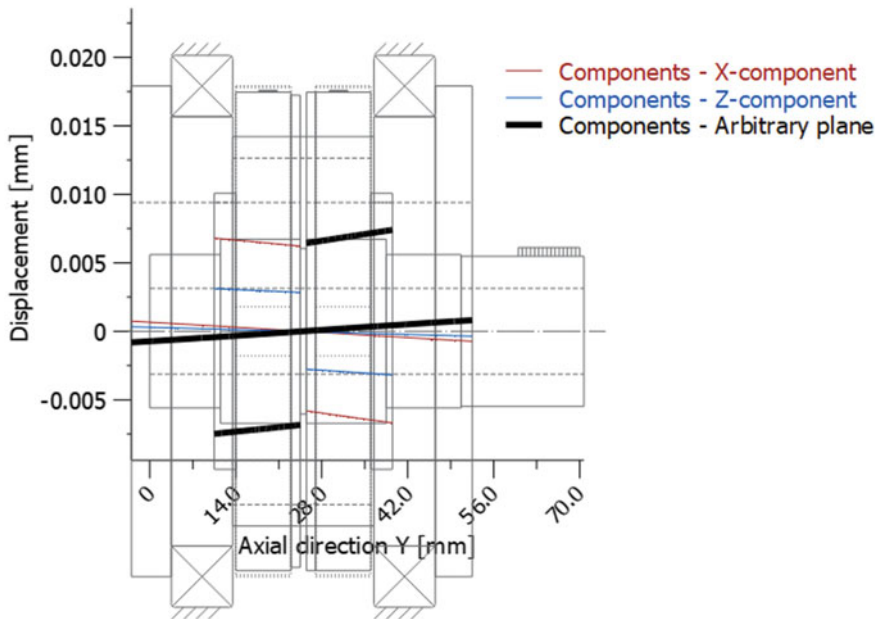


Fig. 14.19 Radial deviation of the planet gear position from the prescribed axis distance

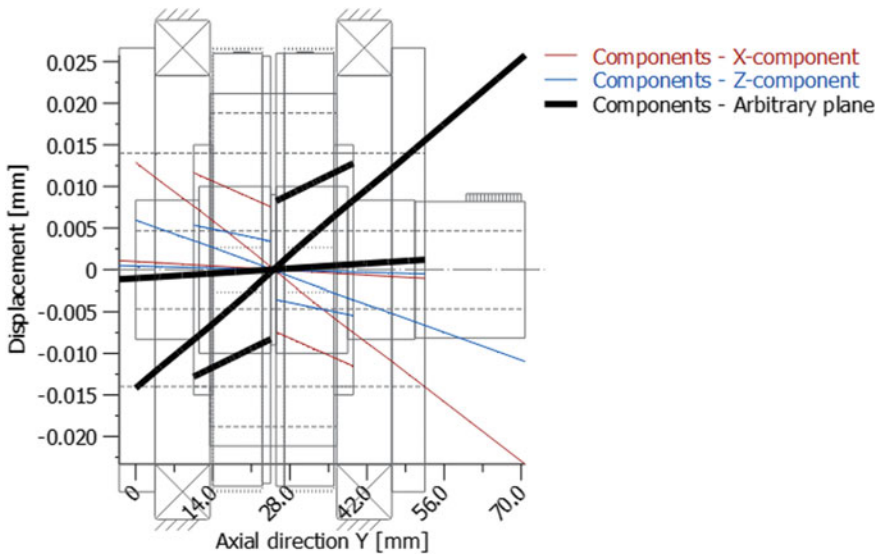


Fig. 14.20 Radial deviation of the planet gear position with increased axis distance deviations

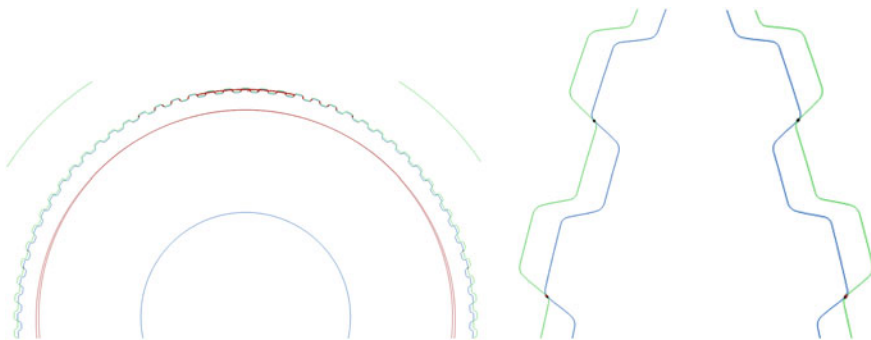


Fig. 14.21 Meshing gear and planet (left) details showing collisions (right)

(left) shows the ring gear and the planet with the already described S-gear geometry ($z_p = 80$, $z_v = 81$). However, Fig. 14.21 (right) clearly shows collisions between the planet and ring gear teeth tips which is located in zones around -70° and $+70^\circ$ from the pitch point. It is necessary to avoid such interferences, and since a near zero backlash can only be achieved with a bit bigger eccentricity (0.520 mm) and with very narrow tooth tolerances the tooth tip rounding must be increased.

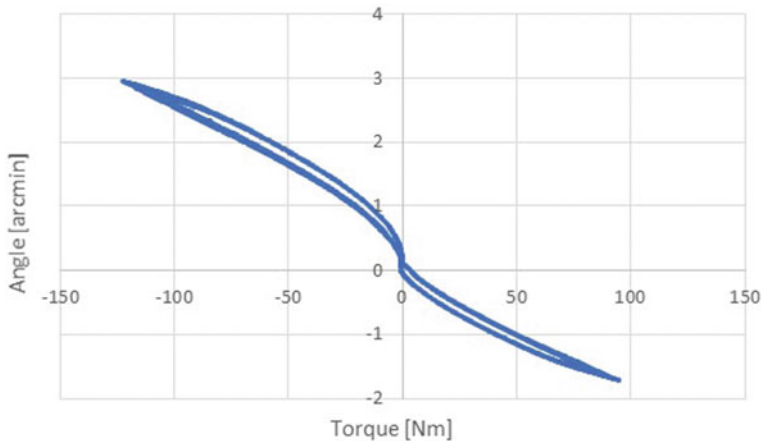


Fig. 14.22 Stiffness and backlash characteristic

14.7 A New Prototype

The next series prototype has been produced, based on the above findings. After CMM inspection of the components, the device was assembled, and its backlash and stiffness characteristic measured by two different methods. First, the testing system induced continuously controlled and measured torque in the range from -120 Nm to $+120$ Nm, Fig. 14.22. The other method is classical, inducing the output torque by a lever and weights. The resulting backlash was in the range of 0.25 arcmin regardless of measurement method.

14.8 Conclusions

The paper describes development of a planocentric gear train based on the S-gearing principles. The gear design enables high gear ratios. However, the produced prototypes exhibited high backlashes and to high vibrations. Design improvements contributed to better performance, but the design aims were not yet met. So, it was necessary to employ analysis of tolerances, contact analysis and radial deviations of the planet gear positions. Careful examination of the findings led to the improved gearing design—with narrow tooth thickness tolerance and bigger tooth tip rounding. The analysis also showed that planet gears and ring gear should be sorted according to their tooth tolerance position. Gears can be fully loaded and at the same time no interference appears. And the most important, the backlash of the gear train developed based on the tolerance analysis is about 0.25 arcmin (Fig. 14.22). Whereas, preliminary results for the stiffness of the system amount to app. 35 Nm/arcmin.

The new series prototypes will be tested in next weeks to disclose their important characteristics, e.g. kinematic error, vibrations and durability tests. A serial production can be prepared based on testing results analysis and a design of a family of products.

Acknowledgements The investment is co-financed by the Republic of Slovenia and the European Union under the European Regional Development Fund, no. SME 2/17-3/2017 and C3330-18-952014



EUROPEAN UNION
EUROPEAN REGIONAL
DEVELOPMENT FUND



REPUBLIC OF SLOVENIA
MINISTRY OF ECONOMIC DEVELOPMENT AND
TECHNOLOGY

References

1. Radzevich, S.P.: *Dudley's Handbook of Practical Gear Design and Manufacture*, Second edn. CRC Press, Taylor & Francis Group, Boca Raton (2012). ISBN 978-1-4398-6602-3 (eBook—PDF)
2. Nieman, G., Winter, H.: *Maschinenelemente, Band II: Getriebe allgemein, Zahnradgetriebe Grundlagen, Stirnrad Getriebe*. Springer, Berlin, Heidelberg, New York. ISBN 3-540-11149-2
3. Sumitomo Drive Technologies: *Fine Cyclo@—Zero Backlash Precision Gear-boxes*, Catalog #991333. www.sumitomodrive.com (2018). Accessed 1 Sept 2019
4. Spinea TwinSpin: *High Precision Reduction Gears*, Ed. I/2017. <https://www.spinea.com/en/products/twinspin/index> (2017). Accessed 1 Sept 2019
5. Nabtesco.: *Precision Reduction Gear RV™* (2018)—E Series/C Series/Original Series CAT.180420. <https://www.nabtesco.de/en/downloads/product-catalogue/>. Accessed 1 Sept 2019
6. Onvio.: *Zero Backlash Speed Reducers*. www.onviollc.com (2005). Accessed 1 Sept 2019
7. Wakida, M., et al.: *Speed change gear and manufacturing method therefor*. Ass. JTEKT Corp., US Patent Application publication, US2011/0245030 A1 (2011)
8. Takuya, H., et al.: *Planetengetriebevorrichtung und Verfahren zur Herstellung einer Planetengetriebevorrichtung*. Anmelder: Sumitomo Heavy Industries, DE Offenlegungsschrift, DE 10 2012 023 988 A1 (2013)
9. Egawa, M.: *Reducer with internally meshing planetary gear mechanism and device incorporating reducer*. Ass.: Sumitomo Heavy Industries, US Patent Application publication, US 2006/0025271 A1 (2006)
10. Stäubli.: *TS2 Robot Range*. <https://www.staubli.com/en/file/21027.show> (2019). Accessed 1 Sept 2019
11. Hlebanja, J., Hlebanja, G.: *Efficiency and maximal transmitted load for internal lantern planetary gears*. In: Fawcett, J.N. (ed.) *International Gearing Conference*, pp. 117–120 (1994)
12. Hlebanja, J., Hlebanja, G.: *Patent No. 9300152, Planetary gear train*. Slovenian Intellectual Property Office (SIPO) (1994)
13. Park, M.-W., et al.: *Development of speed reducer with planocentric involute gearing mechanism*. *J. Mech. Sci. Technol.* **21**(2007), 1172–1177 (2007)
14. Kim, J.H.: *Analysis of planocentric gear*. *Agri. Biosys. Eng.* **7**(1), 13–17 (2006)
15. Nam, W.K., Oh, S.-H.: *A design of speed reducer with trapezoidal tooth profile for robot manipulator*. *J. Mech. Sci. Technol.* **25**(1), 171–176 (2011)

16. Hlebanja, G.: Specially shaped spur gears: a step towards use in miniature mechatronic applications. In: Miltenović, V. (ed.) 7th International Science Conference on Research and Development of Mechanical Elements and Systems—IRMES 2011, Zlatibor, Serbia, Apr 2011. Proceedings, Niš, pp. 475–480 (2011)
17. Hlebanja, G., Hlebanja, J.: Contribution to the development of cylindrical gears. In: Dobre, G., Vladu, M.R. (eds.) Power Transmissions: Proceedings 4th International Conference, Sinaia, Mechanisms and Machine Science, vol. 13, pp. 309–320. Springer, Dordrecht (2013). ISSN 2211-0984
18. Hlebanja, G., Kulovec, S., Hlebanja, J., Duhovnik, J.: S-gears made of polymers. *Ventil* **20**(5), 358–367. ISSN 1318-7279. 10. 2014 (2014)
19. KissSoft.: Design software for mechanical engineering applications. <https://www.kisssoft.ag/english/home/index.php> (2019a) Accessed 23 Sept 2019
20. KissSoft.: KissSoft Release 2019 User Manual. KISSsoft AG—A Gleason Company, Bubikon (2019)